PERGAMON

Electrochimica Acta 47 (2002) 2937–2942

ELECTROCHIMICA Acta

www.elsevier.com/locate/electacta

The effects of Ni and Li doping on the performance of lithium manganese oxide material for lithium secondary batteries

Ki Soo Park [a], Myung Hun Cho [a], Sang Ho Park [b], Kee Suk Nahm [a,*], Yang Kook Sun [b], Yun Sung Lee [c], Masaki Yoshio [c]

[a] *School of Chemical Engineering and Technology, College of Engineering, Chonbuk National University, Chonju 561-756, South Korea*
[b] *Department of Industrial Chemistry, College of Engineering, Hanyang University, Seoul 133-791, South Korea*
[c] *Department of Applied Chemistry, Saga University, 1 Honjo, Saga 840-8502, Japan*

Received 3 December 2001; received in revised form 27 March 2002

Abstract

Layered $Li_{0.7}[M_{1/6}Mn_{5/6}]O_2$ (M = Li, Ni) was synthesized using a sol–gel method. P2-$Na_{0.7}[M_{1/6}Mn_{5/6}]O_2$ precursor was first synthesized by a sol–gel method, and then O2-$Li_{0.7}[M_{1/6}Mn_{5/6}]O_2$ was prepared by an ion exchange of Li for Na in P2-$Na_{0.7}[M_{1/6}Mn_{5/6}]O_2$ precursor. From charge/discharge curves, it was seen that $Li_{0.7}[Li_{1/6}Mn_{5/6}]O_2$ has two plateaus similar to those observed from a spinel structure, but $Li_{0.7}[Ni_{1/6}Mn_{5/6}]O_2$ holds a single plateau as observed from a typical layered structure. It was considered that $Li_{0.7}[Li_{1/6}Mn_{5/6}]O_2$ undergoes a phase transformation from layered to spinel structure during the charge/discharge cycle, but $Li_{0.7}[Ni_{1/6}Mn_{5/6}]O_2$ maintains O2-layered structure after the cycles. $Li_{0.7}[Ni_{1/6}Mn_{5/6}]O_2$ was higher in discharge capacity and retention rate than $Li_{0.7}[Li_{1/6}Mn_{5/6}]O_2$.

Keywords: Sol–gel method; Ni doping; Glycolic acid; Layered structure; Lithium-ion battery

1. Introduction

The explosive demand for portable electronic devices has brought about an increase in the importance of compact, lightweight, and reliable power sources. One of the most probable candidates for such requirements is an Li-ion rechargeable battery, which employs two intercalation compounds for electrode materials. Lithiated transition metal oxides ($LiCoO_2$, $LiNiO_2$, $LiMn_2O_4$) have been extensively studied as cathode materials for commercialization of rechargeable lithium batteries. Among these, spinel lithium manganese oxide ($LiMn_2O_4$) has been considered as a promising candidate for cathode material due to its high intercalation voltage, low cost, abundance, and nontoxicity [1–4]. However, the material has shown a low discharge capacity due to its inherent structure and capacity fading because of its dissolution in the electrolyte, the Jahn–Teller effect, and lattice instability [5–7].

Recently, layered $LiMnO_2$ has been intensively investigated as a new layered cathode material since it has a high theoretical discharge capacity (285 mA h g^{-1}). However, a solid state reaction previously employed to prepare layered $LiMnO_2$ demands high temperatures, which induce the formation of by-product, non-layered structures such as spinel $LiMn_2O_4$, orthorhombic $LiMnO_2$, or rock salt Li_2MnO_3, because layered $LiMnO_2$ is unstable at high temperatures. Therefore, researchers have attempted to prepare layered $LiMnO_2$ by ion exchange of layered alkali bronze A_xMnO_2 (A = K, Na) with lithium.

For layered $LiMnO_2$, which normally forms an O3 structure, the stacking of oxygen atoms follows a cubic close packed (ccp) structure. The $LiMnO_2$ is apt to transform to the stable spinel phase by minor cationic rearrangements, which occur during the first removal and intercalation of Li, leading to the degradation of electrode performance. However, layered Li_xMnO_2 with an O2 structure, which has the most symmetric hexagonal space group $P6_3/mmc$, is thermodynamically

* Corresponding author. Tel.: +82-63-270-2311; fax: +82-63-270-2306
E-mail address: nahmks@moak.chonbuk.ac.kr (K.S. Nahm).

0013-4686/02/$ - see front matter
PII: S0013-4686(02)00186-X

metastable compared with the O3-$LiMnO_2$ structure having space group $C2/m$.

The synthesis of layered Li_xMnO_2 with an O2 structure was studied by Dhan's group using a solid-state reaction [8–13]. They first prepared layered $Na_{0.7}[M_{1/3}Mn_{2/3}]O_2$ with stoichiometric amounts of Mn_2O_3, Li_2CO_3, and Na_2CO_3 using a solid state reaction, and then ion exchanged the prepared P2-$Na_{0.7}[M_{1/3}Mn_{2/3}]O_2$ in a boiling solution of 5 M lithium bromide dissolved in hexanol to form the layered O2 structure. They observed that small deviations cause less ordered samples showing T2–O2 intergrowth structures and reported that the disordered T2 structure obtains the best discharge capacity of about 170 mA h g^{-1} [11]. They also observed doping effects using Li, Ni, and Co. However, the charge/discharge curve differed from existing layered $LiNiO_2$, $LiCoO_2$, etc. The curve shape had two plateaus as shown in the spinel structure.

In this work, we report the synthesis of layered $Li_{0.7}[M_{1/6}Mn_{5/6}]O_2$ (M = Li, Ni) using a sol–gel method. A P2-$Na_{0.7}[M_{1/6}Mn_{5/6}]O_2$ precursor was first synthesized by a sol–gel method, and then O2-$Li_{0.7}[M_{1/6}Mn_{5/6}]O_2$ was prepared by an ion exchange of Li for Na in the P2-$Na_{0.7}[M_{1/6}Mn_{5/6}]O_2$ precursor. The advantage of this method is to synthesize the material at relatively lower temperature for a short time. Ni doping was attempted to enhance the stability of structural and electrochemical properties of the O2 structure. The structural and electrochemical properties of the prepared materials were investigated in this work.

2. Experiment

The P2-$Na_{0.7}[Li_{1/6}Mn_{5/6}]O_2$ precursor was synthesized using a sol–gel method. Sodium acetate (CH_3CO_2Na, Aldrich), lithium acetate ($Li(CH_3COO)\cdot 2H_2O$), and manganese acetate ($Mn(CH_3COO)\cdot 4H_2O$) were employed as starting materials for the synthesis of $Na_{0.7}[Li_{1/6}Mn_{5/6}]O_2$ powder. Stoichiometric amounts of sodium, lithium, and nickel acetate salts were dissolved in DI water with a cationic ratio of Na:Li:Mn = 0.7:1/6:5/6. The dissolved solution was added drop by drop into continuously agitating aqueous glycolic acid. Glycolic acid was employed as a chelating agent in the experiment. The molar ratio of chelating agent to total metal ions was fixed at unity. The pH of the solution was adjusted to be in the range of 8.5–9.5 by adding ammonium hydroxide to the solution. The prepared solution was evaporated at 70–80 °C for 5 h until a transparent sol was obtained. As water evaporated further, the sol turned into a viscous transparent gel. The resulting gel precursors were heated with a ramping rate of 1 °C min^{-1} and decomposed at 450 °C for 10 h in air to eliminate organic components. Thus obtained powders were calcined at the temperature range of 800 °C in a flow of air for 12 h. After the calcination process, the powders were suddenly quenched in liquid N_2. In the case of the P2-$Na_{0.7}[Ni_{1/6}Mn_{5/6}]O_2$ precursor preparation, the process was the same except that nickel acetate ($Ni(CH_3COO)_2\cdot 4H_2O$) salt was used instead of lithium acetate ($Li(CH_3COO)\cdot 2H_2O$).

The prepared precursor powders (5 g) were introduced into a mixed solution of hexanol (150 ml) and lithium bromide (LiBr; 55 g). The ion exchange of Li for Na in $Na_{0.7}[Li_{1/6}Mn_{5/6}]O_2$ was carried out at 160 °C for 3 h under Ar environment in a batch reactor equipped with a reflux condenser to prepare O2-$Li_{0.7}[Li_{1/6}Mn_{5/6}]O_2$. After the reaction, the solution was filtered using an aspirator under vacuum and the remaining powders were washed with methyl alcohol. The washed powders were dried at 180 °C for 10 h in a vacuum oven.

After the synthesis, the amounts of Li, Ni, and Mn in the synthesized materials were analyzed with an induction coupled plasma (ICP) and sulfur analyzer (LECO Co., CS 444), respectively, to determine the real chemical composition of the materials. The oxygen content was determined via mass balance. The chemically analyzed data indicated that the real compositions of $Li_{0.7}[Li_{1/6}Mn_{5/6}]O_2$ and $Li_{0.7}[Ni_{1/6}Mn_{5/6}]O_2$ were $Li_{0.61}[Li_{1/6}Mn_{5/6}]O_2$ and $Li_{0.61}[Ni_{1/6}Mn_{5/6}]O_2$, respectively. The structures of the prepared powders were characterized using powder X-ray diffraction (XRD, D/Max-3A, Rigaku) measurements with Cu–Kα radiation target.

The electrochemical characterization was carried out using CR2032 coin-type cells. The test cells were assembled in the following method: the cathode was fabricated with an accurately weighed active material (20 mg) and conductive binder (13 mg). It was pressed on 25 mm^2 stainless steel mesh used as the current collector at 300 kg cm^{-2} and dried at 200 °C for 5 h in an oven. This cell was composed of a cathode and a lithium metal anode (Cyprus Foote Mineral Co.) separated by a porous polypropylene film used as the separator (Celgard 3401). The electrolyte used was a 1 M $LiPF_6$–ethylene carbonate (EC)/dimethyl carbonate (DMC) (1:2 by volume). The cells were assembled in an argon-filled dry box and tested at room temperature. The cell was charged and discharged at a current density of 0.4 mA cm^{-2} with cut-off voltages from 2.0 V to an upper voltage of 4.2 V (vs. Li/Li^+). After two to three charge/discharge cycles, the upper voltage was sequentially increased by 0.2 until 4.8 V was reached.

3. Results and discussion

Fig. 1 shows typical TGA and DTA curves for P2-$Na_{0.7}[Li_{1/6}Mn_{5/6}]O_2$ gel prepared with a molar ratio of chelating agent to total ions of 1.0. It was observed that

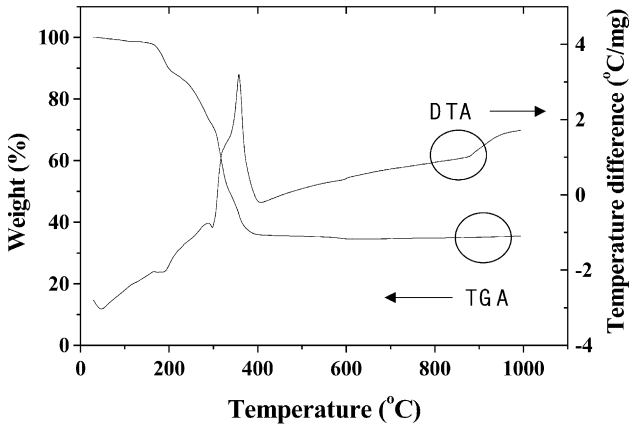

Fig. 1. Thermalgravimetric and differential thermal analysis of the gel. The molar ratio of glycolic acid to the total metal ions was 1.0.

both samples have shown the same behavior in the TGA and DTA measurements. The TGA curve exhibits three distinct weight loss steps and the DTA curve shows one endothermic peak and two exothermic peaks. The first weight loss step in the temperature range of 150–200 °C, which is accompanied by an endothermic peak around 190 °C on the DTA curve, is due to the loss of residual water in the gel. The second weight loss step in the temperature range of 200–400 °C is associated with the decomposition of chelating agent and acetate ions. This pyrolysis behavior has been similarly observed in the syntheses of $LiCoO_2$ [14], $LiNiO_2$ [15] and $LiMn_2O_4$ materials [16].

Fig. 2(a) shows a XRD pattern of $Na_{0.7}[Li_{1/6}Mn_{5/6}]O_2$ powders synthesized at 800 °C using glycolic acid. The asterisks are expressed for characteristic peaks of P3 structure. The (002) peak is observed at $2\theta = 16°$ as a main peak and (012) and (014) peaks appear at $2\theta = 40$ and 49°, respectively, which have been measured from a typical P2 layered structure [9]. Weak peaks of P3 structure are observed at $2\theta = 44$, 53 and 57°, which indicate that the synthesized material includes some P3 structure [11]. Consequently, the synthesized material is considered to have a structure with the most symmetric hexagonal space group structure ($P6_3/mmc$), partially mingled with P3 phase ($C2/m$).

Shown in Fig. 2(b) is a XRD pattern of $Na_{0.7}[Ni_{1/6}Mn_{5/6}]O_2$ powders synthesized at 800 °C using glycolic acid. Differently from Li-doped sodium manganese bronze, this presents no peaks related to P3 structure shown in Fig. 2(a). This means that $Na_{0.7}[Ni_{1/6}Mn_{5/6}]O_2$ powders is solely composed of P2 structure (S.G: $P6_3/mmc$) without impurities.

Fig. 3(a) and (b) show XRD patterns of Li- and Ni-doped lithium manganese oxides prepared by ion exchange of the sodium manganese bronzes. Both the samples experienced a perfect ion exchange without formation of impurities. The (002) peak ($2\theta = 16°$) resulting from Na phase disappears totally, whereas the (002) peak ($2\theta = 18°$) from Li phase appears from the XRD spectra. This indicates that the ion exchange of Li for Na in the sodium manganese bronzes is successfully accomplished in this work. XRD patterns of the two samples exhibit broad characteristic peaks with low intensities, which originate from stacking faults. Stacking faults in layered structures lead to the formation of sharp (00l) and (hk0) peaks in the diffraction patterns [10]. The characteristic peaks with broad FWHM and low intensity are due to the effect of layer gliding in the layered structure when the structure changes from P2 to O2 during ion exchange [17]. Our synthesized samples which exhibit 001 and hk0 peaks with low intensity infer that Li-doped lithium manganese oxide has a layered structure with stacking faults.

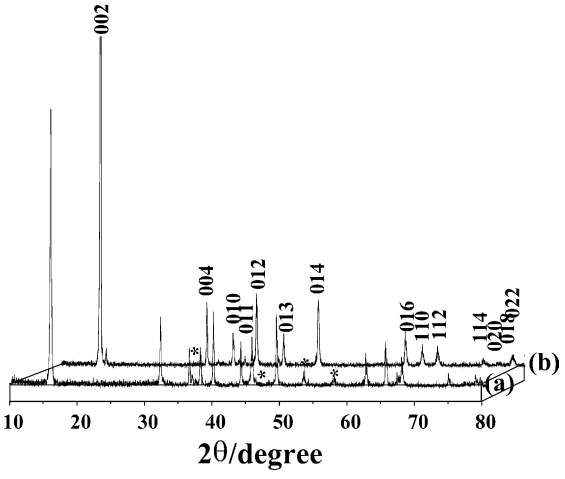

Fig. 2. XRD spectra for (a) Li and (b) Ni-doped $Na_{0.7}[M_{1/6}Mn_{5/6}]O_2$ precursors synthesized using glycolic acids at 800 °C. Asterix peaks (*): unidentified peaks.

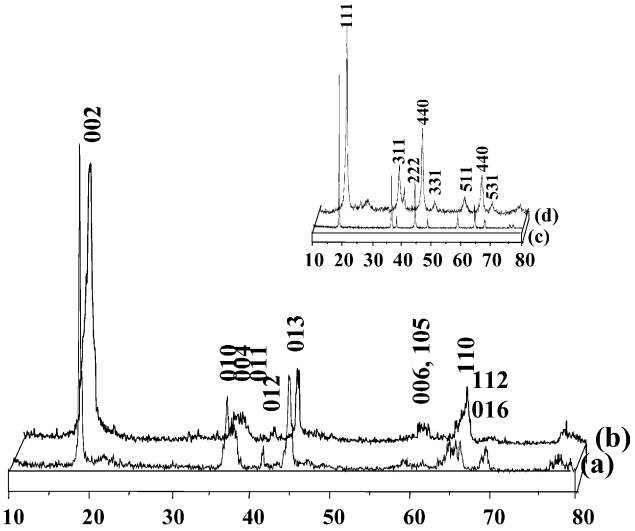

Fig. 3. XRD spectra for (a) Li and (b) Ni-doped $Li_{0.7}[M_{1/6}Mn_{5/6}]O_2$ prepared by ion exchange of Li for Na in sodium manganese oxide precursors synthesized glycolic acids at 800 °C. (c) After cycle, XRD spectrum of Li-doped $Li_{0.7}[M_{1/6}Mn_{5/6}]O_2$ and (d) spinel $LiMn_2O_4$.

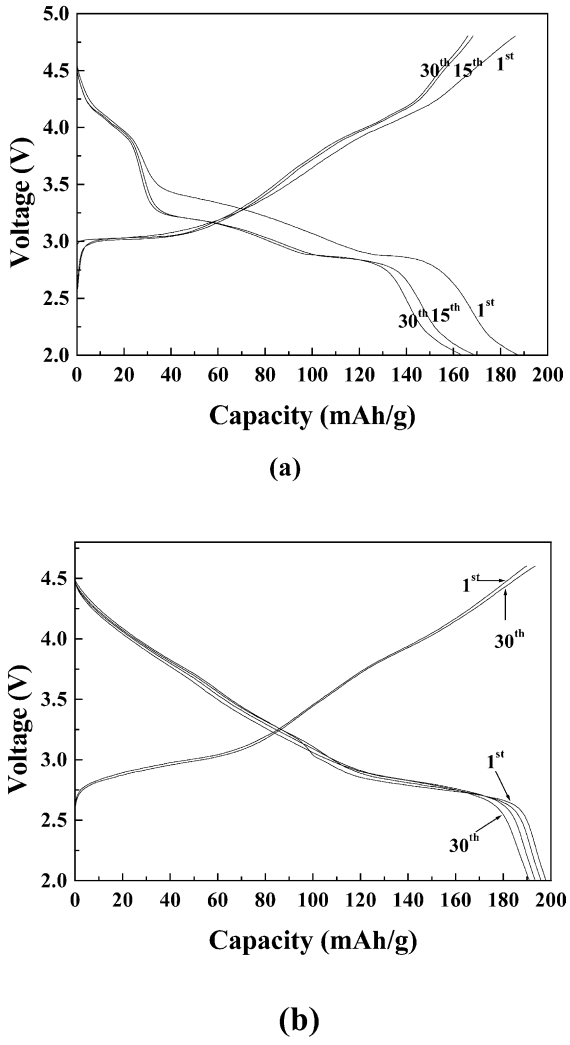

Fig. 4. Charge-discharge curves of $Li_{0.7}[M_{1/6}Mn_{5/6}]O_2$ prepared using glycolic acid; (a) M = Li, (b) M = Ni.

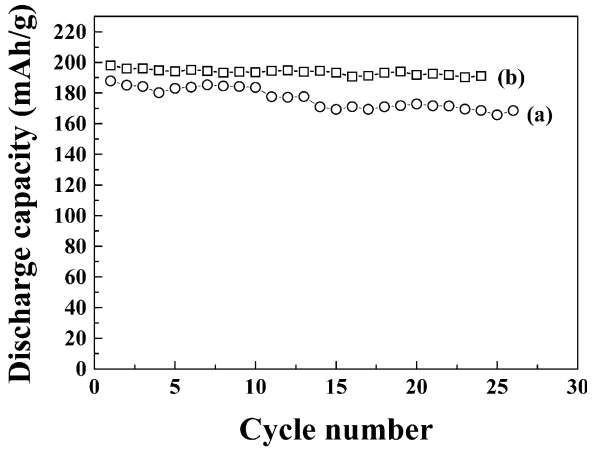

Fig. 5. Plots of specific discharge capacity versus cyclic number for $Li_{0.7}[M_{1/6}Mn_{5/6}]O_2$ prepared using glycolic acid; (a) M = Li, (b) M = Ni.

Fig. 4(a) and Fig. 5(a) show the charge/discharge curves and specific discharge capacity of the Li/$Li_{0.7}[Li_{1/6}Mn_{5/6}]O_2$ cell, respectively. The electrode initially delivers the discharge capacity of 183 mA h g^{-1}, but shows a rapid capacity fading with the cycle at the initial stages. It is observed that with increasing cycle number a typical discharge curve shape of the spinel structure becomes valid from the discharge curve of the $Li_{0.7}[Li_{1/6}Mn_{5/6}]O_2$ electrode. The discharge curve of the $Li_{0.7}[Li_{1/6}Mn_{5/6}]O_2$ electrode shows two distinct plateaus at around 4 and 3 V, which are generally observed from a spinel-type manganese oxide. This means that the $Li_{0.7}[Li_{1/6}Mn_{5/6}]O_2$ material undergoes the structural transition from layered to spinel like structure during the charge/discharge cycle. The structure of $Li_{0.7}[Li_{1/6}Mn_{5/6}]O_2$ material was evaluated after charge/discharge cycling to see structural transition from layered to spinel like structure. Fig. 3(c) shows the XRD pattern for the $Li_{0.7}[Li_{1/6}Mn_{5/6}]O_2$ electrode cycled after 30th cycle with a typical XRD spectrum of spinel $LiMn_2O_4$. Although as-prepared $Li_{0.7}[Li_{1/6}Mn_{5/6}]O_2$ powders showed the formation of layered lithium manganese oxide (Fig. 3(a)), Fig. 3(c) obviously shows the formation of the spinel structure, which is similar to a typical XRD spectrum of spinel $LiMn_2O_4$, as shown in Fig. 3(d) [18]. This proves the $Li_{0.7}[Li_{1/6}Mn_{5/6}]O_2$ undergoes a structural change from layered to spinel like structure during the cycle.

From Fig. 5(a), it is seen that the electrode attains a good cycling behavior while retaining 93% (0.65 mA h g^{-1} cycle) of the initial capacity after 25 cycles at C/3 rate. It is very interesting to note that our prepared sample shows a good retention rate although its structure changes to spinel structure. It has been generally reported that the discharge capacity of spinel lithium manganese oxides decreases significantly with increasing cycle number [19–21]. As reported in some previous literature, however, this sample does not decrease its discharge capacity although the structure is transited to spinel-like phase [17,22]. They reported that layered lithium manganese oxides attain a high discharge capacity with a low capacity fading although their structure transforms to a spinel-like phase with cycling. Quine and coworkers reported that layered $Li_xMn_{1-y}Ni_yO_2$ with O3 (α-$NaFeO_2$) structure delivers a high capacity of 220 mA h g^{-1} in the voltage 2.4–4.8 V [17]. After the cycling, however, the electrode seemed to have a phase transformation to a spinel-like structure. Amstrong et al. also reported that the structural transition from layered to spinel structure does not appear to have a deleterious effect on the cycling performance of layered $Li[Mn_{1-y}Co_y]O_2$ cathode material [22].

Fig. 4(b) and Fig. 5(b) present the charge/discharge curves and discharge capacity of the Li/$Li_{0.7}[Ni_{1/6}Mn_{5/6}]O_2$ cell, respectively. In the case of Ni-

doped lithium manganese oxide, the electrochemical characteristics of the $Li_{0.7}[Ni_{1/6}Mn_{5/6}]O_2$ was different from that of $Li_{0.7}[Li_{1/6}Mn_{5/6}]O_2$. The discharge curve of $Li_{0.7}[Ni_{1/6}Mn_{5/6}]O_2$ shows a single plateau as observed from the layered structures such as $LiNiO_2$ and $LiCoO_2$ [23–26]. It seemed from Fig. 4(a) that $Li_{0.7}[Li_{1/6}Mn_{5/6}]O_2$ prepared at 800 °C using glycolic acid forms a relatively unstable structure, and accordingly undergoes the structural transition to spinel from layered structure during the cycles. However, Ni-doped $Li_{0.7}[Ni_{1/6}Mn_{5/6}]O_2$ prepared under the same conditions seems to form a comparatively stable O2-structure. The charge/discharge curve shows a typical shape as observed from the layered structures and the change of the curve shape was not detected during the cycles. This means that $Li_{0.7}[Ni_{1/6}Mn_{5/6}]O_2$ maintains O2-layered structure even after several cycles and forms a stable O2-structure. Although not presented in this paper, XRD measurement of $Li_{0.7}[Li_{1/6}Mn_{5/6}]O_2$ electrodes cycled after 30th cycle showed no change in the XRD pattern, indicating that $Li_{0.7}[Ni_{1/6}Mn_{5/6}]O_2$ maintains O2-layered structure after the cycles. This sample delivers the first discharge capacity of 198 mA h g^{-1} between 4.6 and 2.0 V and shows an excellent cycling behavior while retaining 96% (0.32 mA h g^{-1}·cycle) of the initial capacity after 25 cycles at C/3 rate. The initial discharge capacity and retention ratio of Ni-doped sample is higher than those of Li-doped sample.

Figs. 6 and 7 show slow sweep cyclic voltammograms of the $Li_{0.7}[Li_{1/6}Mn_{5/6}]O_2$ and $Li_{0.7}[Ni_{1/6}Mn_{5/6}]O_2$ with a scan rate of 0.1 mV s^{-1} between a potential range of 2.0 and 4.6 V, respectively. The cyclic voltammogram of a spinel $LiMn_2O_4$ is presented together in the figures for comparison. In order to investigate distinctly the structural transition of the materials with cycle, the magnified curves in the voltage region of 3.5–4.5 V are depicted in Fig. 8. As shown in Fig. 6, from $Li_{0.7}[Li_{1/6}Mn_{5/6}]O_2$, oxidation peaks are clearly observed at 2.85 and 3.9 V, whereas the reduction peaks appear at 2.75 and 3.9 V. The most important feature in the figure is that only one reduction peak presents at 3.9 V up to the 1st cycle, but another reduction peak begins to grow up at 4.1 V from the 2nd cycle. The characteristic electrochemical properties of spinel phase $Li_xMn_2O_4$ is that Li is inserted into tetrahedral sites over the 4 V plateau corresponding to $0 < x \leq 1$, and into the octahedral sites over the 3 V plateau corresponding to $1 \leq x \leq 2$ [27]. The 4 V plateau shows a two-step profile at 4.02 and 4.2 V during the charge and at 3.95 and 4.05 V during discharge [27–29], as also observed from Fig. 8. Therefore, the appearance of a reduction peak at 4.1 V from the 2nd cycle means the Li-doped sample undergoes the structural transformation from layered to spinel-like structure during electrochemical cycling.

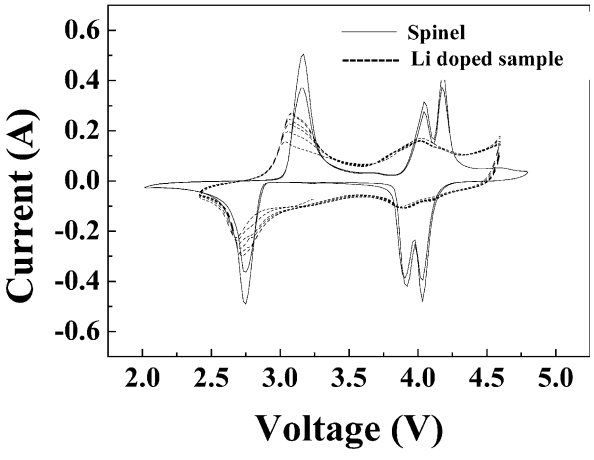

Fig. 6. The cyclic voltamograms recorded at scan rate of 0.1 mV s^{-1} between potential range of 2.0 and 4.6 V for $Li_{0.7}[Li_{1/6}Mn_{5/6}]O_2$ with $LiMn_2O_4$.

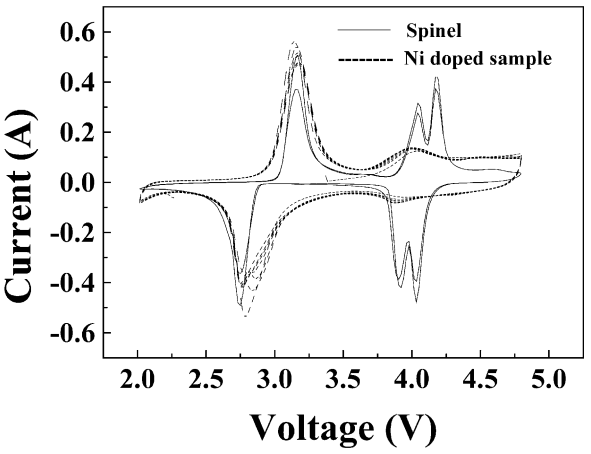

Fig. 7. The cyclic voltamograms recorded at scan rate of 0.1 mV s^{-1} between potential range of 2.0 and 4.6 V for $Li_{0.7}[Ni_{1/6}Mn_{5/6}]O_2$ with $LiMn_2O_4$.

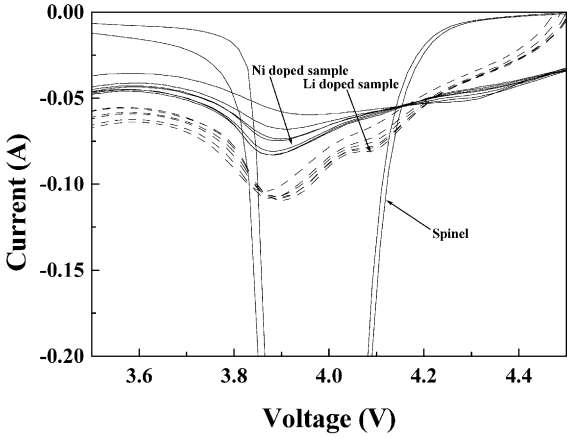

Fig. 8. The magnified cyclic voltamograms curves in the voltage region of 3.5–4.5 V for $Li_{0.7}[Li_{1/6}Mn_{5/6}]O_2$ and $Li_{0.7}[Ni_{1/6}Mn_{5/6}]O_2$ with $LiMn_2O_4$.

The areas under the two redox peaks were almost equal. These results indicate that the intercalation/deintercalation of Li ions occur in a two stage process and are reversible in the material.

For the Ni-doped sample, however, it shows a different curve shape from the Li-doped sample. The sample evolves only one peak at 3.9 V without the evolution of a peak at 4.1 V although the cycle number increases. This means that the Ni-doped sample does not undergo the phase transition from layered to spinel structure.

4. Conclusion

$Li_{0.7}[M_{1/6}Mn_{5/6}]O_2$ (M = Li, Ni) powders have been prepared by the ion exchange of Li for Na in $Na_{0.7}[M_{1/6}Mn_{5/6}]O_2$ precursor synthesized by a sol–gel method using glycolic acid. Li-doped and Ni-doped $Li_{0.7}[M_{1/6}Mn_{5/6}]O_2$ showed two plateaus and one plateau on the discharge curves, respectively. Meanwhile, they delivered the discharge capacities of 183 and 198 mA h g^{-1}, respectively, at the first cycle. The retention ratio of Ni-doped sample (96% (0.32 mA h g^{-1}·cycle)) was higher than that of Li-doped sample (93% (0.65 mA h g^{-1}·cycle)). The charge/discharge curve shape of the $Li_{0.7}[Li_{1/6}Mn_{5/6}]O_2$ electrode was similar to that of the spinel structure, resulting in the phase change to the spinel-like structure during the cycle. However, the $Li_{0.7}[Ni_{1/6}Mn_{5/6}]O_2$ electrode showed the typical shape the layered structures generally have and exhibited no phase change during the cycle.

Acknowledgements

This work is supported by the Ministry of Information & Communication of Korea ('Support Project of University Information Technology Research Center' supervised by KIPA).

References

[1] M.D. Levi, K. Gamolsky, D. Aubach, U. Heider, R. Oesten, J. Electrochem. Soc. 147 (2000) 25.
[2] M.M. Thackeray, in: R.T. Brodd (Ed.), Programme, Batteries Battery Material, Lithium Ion Battery Technology, vol. 141, ITE-JES Press, OH, 1995, p. 1.
[3] Y.K. Sun, Y.S. Jeon, J. Mater. Chem. 9 (1999) 3147.
[4] Y.K. Sun, Electrochem. Commun. 2 (2000) 6.
[5] G.G. Amatucci, C.N. Schmutz, A. Bylr, C. Siala, A.S. Gozdz, D. Larcher, J.-M. Tarascon, J. Power Sources 69 (1997) 11.
[6] Y. Xia, Y. Zhou, M. Yoshio, J. Electrochem. Soc. 144 (1997) 2593.
[7] H. Huang, C.A. Vincent, P.G. Bruce, J. Electrochem. Soc. 146 (1999) 481.
[8] J.M. Paulsen, J.R. Dahn, Solid State Ionics 126 (1999) 3.
[9] J.M. Paulsen, C.L. Thomas, J.R. Dahn, J. Electrochem. Soc. 3560 (1999) 146.
[10] J.M. Paulsen, C.L. Thomas, J.R. Dahn, J. Electrochem. Soc. 861 (2000) 147.
[11] J.M. Paulsen, J.R. Dahn, J. Electrochem. Soc. 2478 (2000) 147.
[12] J.M. Paulsen, D. Larcher, J.R. Dahn, J. Electrochem. Soc. 2862 (2000) 147.
[13] Z. Lu, R.A. Donaberger, J.R. Dahn, Chem. Mater. 3583 (2000) 12.
[14] Y.K. Sun, I.H. Oh, S.A. Hong, J. Mater. Sci. 3617 (1996) 31.
[15] S.H. Park, K.S. Park, Y.K. Sun, K.S. Nahm, Y.S. Lee, M. Yoshio, Electrochem. Acta 1215 (2001) 26.
[16] Y.K. Sun, I.H. Oh, K.Y. Kim, Ind. Eng. Chem. Res. 4839 (1997) 36.
[17] T.E. Quine, M.J. Duncan, A.R. Armstrong, A.D. Robertson, P.G. Bruce, J. Mater. Chem. 10 (2000) 2838.
[18] S.H. Park, K.S. Park, S.S. Moon, Y.K. Sun, K.S. Nahm, J. Power Sources 92 (2001) 244.
[19] M. Okada, Y.S. Lee, M. Yoshio, J. Power Sources 90 (2000) 196.
[20] G.X. Wang, D.H. Bradkurst, H.K. Liu, S.X. Dou, Solid State Ionics 120 (1999) 95.
[21] N. Hayashi, H. Ikuta, M. Wakihara, J. Electrochem. Soc. 146 (1999) 1351.
[22] A.R. Armstrong, A.D. Robertson, P.G. Bruce, Electrochim. Acta 45 (1999) 285–294.
[23] S.H. Park, K.S. Park, Y.K. Sun, K.S. Nahm, J. Electrochem. Soc. 2116 (2000) 147.
[24] H. Wang, Y.I. Jang, B. Huang, D.R. Sadoway, Y.M. Chaing, J. Power Soc. 594 (147) (1999) 82.
[25] J.S. Hong, J.R. Selman, J. Electrochem. Soc. 3183 (2000) 147.
[26] K.K. Lee, K.B. Kim, J. Electrochem. Soc. 1709 (2000) 147.
[27] M.M. Thackeray, Prog. Solid State Chem. 25 (1997) 1.
[28] T. Ohzuku, M. Kitaagawa, T. Hirai, J. Electrochem. Soc. 137 (1990) 769.
[29] T. Ohzuku, M. Kitaagawa, T. Hirai, J. Electrochem. Soc. 146 (1999) 3217.